Ground-state properties of the two-site Hubbard–Holstein model: an exact solution

2009 J. Phys.: Condens. Matter 21 415601

(http://iopscience.iop.org/0953-8984/21/41/415601)

J. Phys.: Condens. Matter **21** (2009) 415601 (7pp) doi:10.1088/0953-8984/21/41/415601

Ground-state properties of the two-site Hubbard–Holstein model: an exact solution

Yu-Yu Zhang[1,2], Tao Liu[3], Qing-Hu Chen[2,1,5], Xiaoguang Wang[1] and Ke-Lin Wang[3,4]

[1] Department of Physics, Zhejiang University, Hangzhou 321004, People's Republic of China
[2] Center for Statistical and Theoretical Condensed Matter Physics, Zhejiang Normal University, Jinhua 321004, People's Republic of China
[3] Department of Physics, Southwest University of Science and Technology, Mianyang 621010, People's Republic of China
[4] Department of Modern Physics, University of Science and Technology of China, Hefei 230026, People's Republic of China

E-mail: qhchen@zju.edu.cn

Received 7 July 2009, in final form 1 September 2009
Published 23 September 2009
Online at stacks.iop.org/JPhysCM/21/415601

Abstract
We study the two-site Hubbard–Holstein model by using an extended phonon coherent state. For the nontrivial singlet bipolarons, the double occupancy probability, the fidelity and the entanglement entropy are calculated to characterize the ground-state properties in both two-site and single-site bipolaron-dominated regimes. We use the localized minimum of the fidelity to define a crossover and plot the bipolaron phase diagram, which separates the large and small entanglement region. Furthermore, the relation between the bipolaron entanglement and the correlation functions demonstrates that the large entanglement corresponds to the large magnitude of lattice deformations induced by electrons.

1. Introduction

Recently, contemporary alternative characterizations of the ground-state (GS) properties have been focused on quantum information tools in terms of quantum entanglement [1–5] and fidelity [6–15], which will establish a somewhat interesting understanding from the field of quantum information theory to condensed matter physics. The entanglement entropy, no doubt, quantifies the strength of quantum correlations between subsystems of a compound system. More recently, the crossover characterizing the GS properties of the attractive Bose–Hubbard model [14] and the BCS Bose–Einstein condensation crossover [16] are investigated in terms of the fidelity. It is thus expected that the fidelity is able to furnish a signature of the bipolaron crossover in the electron–phonon coupling systems.

While most of the work in this relatively new field focuses on several concrete models, such as spin models [3, 8, 11, 17, 18] or fermionic models [4, 9, 19, 20], the significant Hubbard–Holstein (HH) model went somewhat unaddressed so far due to a computational challenge [21–27]. Motivated by this, we investigate a simplified two-site HH model, where two electrons hop between two adjacent lattice sites. It is not only a prototype of the HH model but also helpful to better understand the interesting problem of what happens when the electron–electron (e–e) interactions coexist with the electron–phonon (e–ph) interaction. We are interested in the insight provided by observables borrowed from quantum information theory. The fidelity is expected to detect the different bipolaron regions driven by the competition between the e–e and e–ph interactions. The entanglement entropy, in the presence of the quantum correlation, is exploited to quantify bipartite entanglement between electrons and their environment phonons. Despite this simple model having been previously investigated by the variational method [28, 29], numerical diagonalization [30, 31] and Green's functions solution [32], the exact GS wavefunction is still an obstacle in the calculation of the GS fidelity and entanglement entropy.

The extended bosonic coherent state approach was recently successfully addressed in many-body systems [5, 33–35].

[5] Author to whom any correspondence should be addressed.

In this work, we develop this concise technique to deal with the two-site HH model exactly. The advantage of this exact solution is that the wavefunction is proposed explicitly, by which the GS fidelity and the entanglement entropy can be calculated directly. This paper is organized as follows. In section 2 we introduce the model and describe the approach. In section 3, from the quantum information perspective, we calculate the GS fidelity and its susceptibility, the linear entropy and its relation with the correlation function to study crossover properties. The main conclusions are given in section 4.

2. Hamiltonian and solution

The Hamiltonian of the two-site HH model takes the form

$$H = \sum_{i,\sigma} \varepsilon n_{i\sigma} - \sum_{\sigma} t(c_{1\sigma}^{\dagger} c_{2\sigma} + \text{H.c.}) + U \sum_{i} n_{i\uparrow} n_{i\downarrow} + V n_1 n_2 + g_1\omega_0 \sum_{i,\sigma} n_{i,\sigma}(b_i + b_i^{\dagger}) + g_2\omega_0 \sum_{i,\sigma} n_{i,\sigma}(b_{i+\delta} + b_{i+\delta}^{\dagger}) + \omega_0 \sum_{i} b_i^{\dagger} b_i, \quad (1)$$

where $i\,(=1 \text{ or } 2)$ denotes the label of sites. $i+\delta = 2$ for $i = 1$ and vice versa. $c_{i\sigma}\,(c_{i\sigma}^{\dagger})$ annihilates (creates) an electron at site i with σ, and $n_{i,\sigma}(=c_{i\sigma}^{\dagger} c_{i\sigma})$ are electron number operators. ε is the unperturbed site potential. t is the usual hopping integral. U and V denote the on-site and inter-site Coulomb repulsion between electrons, respectively. g_1 and g_2 denote the on-site and inter-site e–ph coupling parameters. $b_i\,(b_i^{\dagger})$ is the annihilation (creation) operator of the local phonon mode at site i. ω_0 is the phonon frequency and is set to unity for convenience.

Introducing new phonon operators $a = (b_1 + b_2)/\sqrt{2}$ and $d = (b_1 - b_2)/\sqrt{2}$, the Hamiltonian (1) can be written in two independent parts ($H = H_d + H_a$):

$$H_d = d^{\dagger} d + \sum_{i,\sigma} \varepsilon n_{i\sigma} - \sum_{\sigma} t(c_{1\sigma}^{\dagger} c_{2\sigma} + \text{H.c.}) + V n_1 n_2 + U \sum_{i} n_{i\uparrow} n_{i\downarrow} + g_-(n_1 - n_2)(d + d^{\dagger}) - n^2 g_+^2 \quad (2)$$

and $H_a = \tilde{a}^{\dagger}\tilde{a}$, where $\tilde{a}^{\dagger} = a^{\dagger} + n g_+$, $\tilde{a} = a + n g_+$, $g_+ = (g_1 + g_2)/\sqrt{2}$ and $g_- = (g_1 - g_2)/\sqrt{2}$. H_a describes a shifted oscillator and represents lowering of energy, which is a constant motion. H_d represents an effective e–ph coupling system whose phonons are coupled linearly with the electrons.

As illustrated in the previous work [28, 32], the triplet two-electron eigenstates of the effective Hamiltonian H_d is trivial and we ignore these states in the following. In terms of the singlet electron state $c_{1\uparrow}^{\dagger} c_{1\downarrow}^{\dagger}|0\rangle_{\text{e}}$, $c_{2\uparrow}^{\dagger} c_{2\downarrow}^{\dagger}|0\rangle_{\text{e}}$ and $\frac{1}{\sqrt{2}}(c_{1\uparrow}^{\dagger} c_{2\downarrow}^{\dagger} - c_{1\downarrow}^{\dagger} c_{2\uparrow}^{\dagger})|0\rangle_{\text{e}}$, the bipolaronic wavefunction $|\psi\rangle$ is expressed as

$$|\psi\rangle = |\varphi_1\rangle c_{1\uparrow}^{\dagger} c_{1\downarrow}^{\dagger}|0\rangle_{\text{e}} + |\varphi_2\rangle c_{2\uparrow}^{\dagger} c_{2\downarrow}^{\dagger}|0\rangle_{\text{e}} + |\varphi_3\rangle \frac{1}{\sqrt{2}}(c_{1\uparrow}^{\dagger} c_{2\downarrow}^{\dagger} - c_{1\downarrow}^{\dagger} c_{2\uparrow}^{\dagger})|0\rangle_{\text{e}}, \quad (3)$$

where $|\varphi_1\rangle$, $|\varphi_2\rangle$ and $|\varphi_3\rangle$ correspond to phonon states. Inserting it into a Schrödinger equation for the effective Hamiltonian in equation (2), it yields

$$[A^{\dagger} A + 2\varepsilon - 4(g_1^2 + g_2^2) + U]|\varphi_1\rangle - \sqrt{2}t|\varphi_3\rangle = E|\varphi_1\rangle \quad (4)$$

$$[B^{\dagger} B + 2\varepsilon - 4(g_1^2 + g_2^2) + U]|\varphi_2\rangle - \sqrt{2}t|\varphi_3\rangle = E|\varphi_2\rangle \quad (5)$$

$$[d^{\dagger} d + 2\varepsilon - 2(g_1 + g_2)^2 + V]|\varphi_3\rangle - \sqrt{2}t(|\varphi_1\rangle + |\varphi_2\rangle) = E|\varphi_3\rangle \quad (6)$$

where we have used two displacement transformations $A^{\dagger} = d^{\dagger} + 2g_-$ and $B^{\dagger} = d^{\dagger} - 2g_-$. Note that the linear term for the phonon operator $d(d^{+})$ is removed and two new free bosonic fields with operators $A(A^{+})$ and $B(B^{+})$ appear. In terms of the basis of these new operators, the phonon states can be expressed as $|\varphi_1\rangle = \sum_{n=0}^{N_{\text{tr}}} f_{1n}(A^{+})^n|0\rangle_A$ and $|\varphi_2\rangle = \sum_{n=0}^{N_{\text{tr}}} f_{2n}(B^{+})^n|0\rangle_B$, where N_{tr} is the truncated boson number. As we know the vacuum state $|0\rangle_{A(B)} = \text{e}^{\mp 2g_- d^{\dagger} - 2g_-^2}|0\rangle$ is just a bosonic coherent state in $d(d^{+})$ with an eigenvalue $-2g_-(2g_-)$ [33–35]. So this new basis is overcomplete and actually does not involve any truncation in the Fock space of $d(d^{+})$, which highlights the present approach. It is also clear that many-body correlations for bosons are essentially included in extended coherent states $|\varphi_1\rangle$ and $|\varphi_2\rangle$. As usual, the phonon state $|\varphi_3\rangle = \sum_{n=0}^{N_{\text{tr}}} f_{3n}(a^{+})^n|0\rangle$ is expanded in a complete basis $|n\rangle$, which is the Fock state of $d(d^{+})$.

Based on these coherent phonon states, we can explicitly solve the Schrödinger equations in equations (4)–(6) by the numerical diagonalization method in dimensions $3N_{\text{tr}} \times 3N_{\text{tr}}$. To obtain the true accurate results, in principle, the truncated number N_{tr} should be taken to infinity. As reported in detail in [5], bosons N_{tr} can be added step by step until further corrections will not change the results. In the present calculation, $N_{\text{tr}} = 30$ is large enough to give very accurate results with a relative error less than 10^{-6} in the whole parameter range. It should be noted that in the exact diagonalization in the Fock space of the original phonon state d [31], a considerably large phonon number is needed to give reasonably good results. We believe that we have exactly solved this model numerically.

To show the effectiveness of the present approach, we first calculate the GS energy. Figure 1(a) presents the GS energy E_0/t as a function of the on-site effective coupling strength $\lambda = g_1^2/t$ by setting $g_2 = 0$ conveniently. The results for the energy by the variational method based on the modified Lang–Firsov transformation with a squeezing phonon state transformation (MLFS) [28] are also listed. It is observed that the present results are lower than the MLFS results [28], especially in the intermediate coupling regime. Comparing with figure 1(a) in [32], we find that the present results for the GS energy are consistent with those from the lowest pole of Green's function.

3. Ground-state properties

3.1. Crossover from two-site to single-site bipolarons

As shown in figure 1(a) there are two distinct regimes. In [32], the energy versus λ curves in the two regimes are fitted by two functions, and the abrupt drop of the first-order derivative signals the crossover regime from two-site bipolarons to single-site bipolarons. We will propose a quantitative criterion. Because the exact wavefunction in the present technique is explicitly given, we can first calculate the probability of the

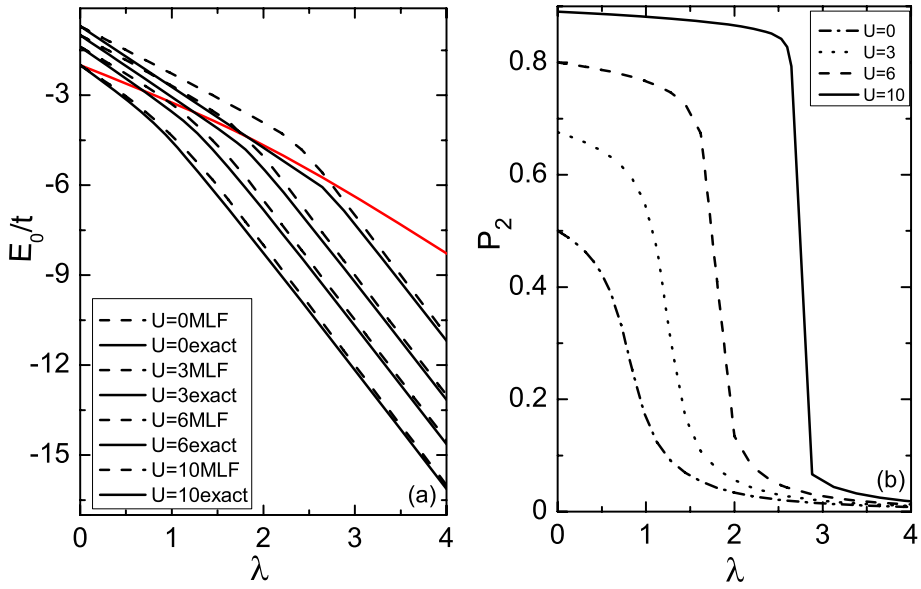

Figure 1. (a) GS energy E_0/t of the exact solution (solid line) and MLFS transformation (dashed line) versus λ for $U = 0, 3, 6$ and 10. The red line represents twice the polaron GS energy, which then separates the polaron and bipolaron regimes. (b) The probability of the two-site bipolarons P_2 for $U = 0, 3, 6$ and 10. The other parameters are chosen: $V = 0, t = 2.0, \varepsilon = 0$.

system that two electrons are in two sites by equation (6) directly:

$$P_2 = \langle\varphi_3|\varphi_3\rangle. \tag{7}$$

The probability of the two-site bipolarons P_2 is shown in figure 1(b). At the weak coupling, the two electrons prefer to stay in two sites. As the coupling strength increases, the two electrons tend to occupy the single site. Strictly speaking, at weak (strong) coupling, pure two-site (single-site) bipolarons do not exist. We can only say that two-site (single-site) bipolarons dominate. The crossover regime is wide for weak on-site Coulomb repulsion U. As U increases, the crossover shifts to larger λ and becomes sharper. However, the sudden jump of P_2 is not observed.

The inter-site Coulomb repulsion V may favor the formation of single-site bipolarons. To show this effect, we calculate the GS energy and the probability of the two-site bipolarons for several values of V for fixed U, which are displayed in figure 2. It is clear that the crossover shifts to smaller λ with increasing V and becomes smoother. It should be pointed out that further consideration of the inter-site Coulomb repulsion V will not yield additional effort mathematically, because the coefficient V can be absorbed in U for the two-site case.

The bipolaron problem in the HH model in many sites was studied numerically by Wellein *et al* [26] and Bonča *et al* [27] many years ago. It was found that a transition (crossover) from inter-site bipolarons, equivalent to the two-site bipolaron in our two-site model, to the on-site bipolaron occurs as the electron–phonon coupling increases. It is interesting to note that the present observation is consistent with the previous picture for the HH model in many sites.

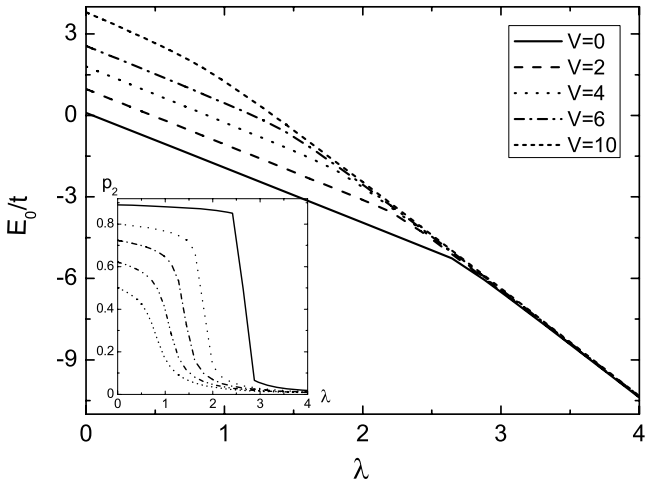

Figure 2. GS energy E_0/t and the probability of the two-site bipolarons P_2 in the inset versus λ for $V = 0, 2, 4, 6$ and 10 by choosing $U = 0.2, t = 2.0$ and $\varepsilon = 0.8$.

3.2. Crossover properties from a quantum information perspective

As we mentioned, the fidelity, which emerged from the perspective of the GS wavefunctions [8, 12], is expected to provide insight into the interplay between the e–ph coupling and e–e Coulomb repulsion. A simple expression of the fidelity $F(g_1, g_1 + \delta g_1)$ is given just by the modulus of the overlap [9]:

$$F = |\langle\varphi_1(g_1)|\varphi_1(g_1 + \delta g_1)\rangle + \langle\varphi_2(g_1)|\varphi_2(g_1 + \delta g_1)\rangle + \langle\varphi_3(g_1)|\varphi_3(g_1 + \delta g_1)\rangle| \tag{8}$$

where $|\psi(g_1)\rangle$ and $|\psi(g_1 + \delta g_1)\rangle$ are two normalized GS corresponding to neighboring Hamiltonian parameters. While

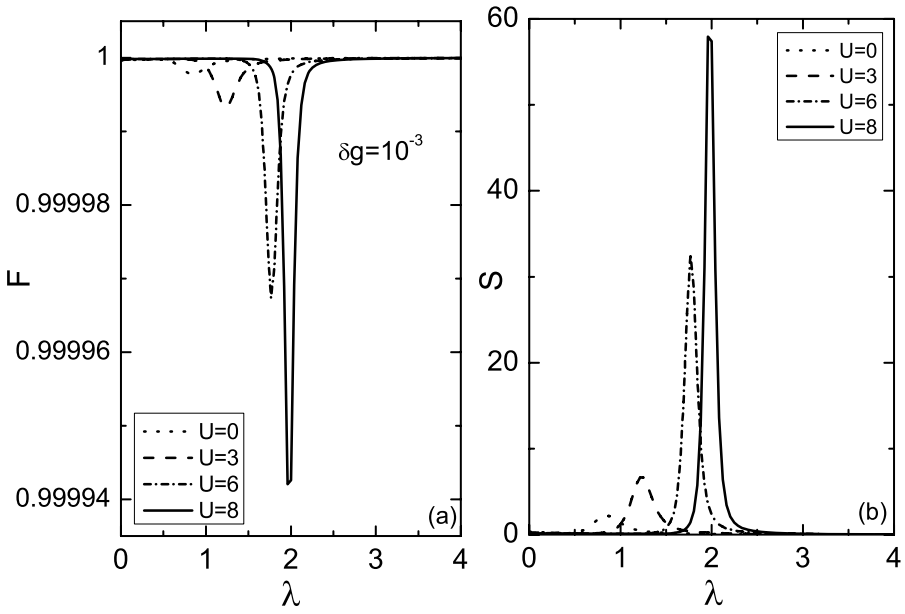

Figure 3. GS fidelity F and its susceptibility S versus λ for $U = 0, 3, 6, 8$ by choosing $V = 0.2$, $t = 2.0$ and $\varepsilon = 0.8$.

the fidelity susceptibility $S(g_1)$ is regarded as a more effective tool, because it is independent of the arbitrary small amount of the parameter δg_1:

$$S(g_1) = \lim_{\delta g_1 \longrightarrow 0} [1 - F(g_1, g_1 + \delta g_1)]/(\delta g_1^2). \qquad (9)$$

We first calculated the GS fidelity F as a function of effective coupling strength λ for different e–e Coulomb repulsion U, as shown in figure 3(a). In our calculations, $\delta g_1 = 10^{-3}$ is used. As is evident, a smooth drop around a certain value $\lambda_{\min}$ is observed, which separates the two-site and singlet-site bipolaron-dominated regions. An occurrence of a localized minimum of the fidelity can be regarded as a signature for the crossover, where the intrinsic properties of the wavefunction changes considerably. Note that the values of the GS fidelity are around 1 in the two limits. For the first-order quantum phase transition system, the GS wavefunctions from different sides of the level-crossing point are almost orthogonal [8]. However, there is an absence of the level crossing and then values of peaks of the GS fidelity are around 1 rather than 0 in the crossover regime. Further evidence for this crossover is given by the susceptibility S, which shows a peak in the intermediate coupling regime in figure 3(b). Obviously, the crossover becomes sharper and $\lambda_{\min}$ is larger as the e–e Coulomb repulsion U increases. It implies that the two-site to single-site bipolaron transition is suppressed by the e–e Coulomb repulsion. The corresponding U/t–λ phase diagram is displayed in figure 4 using the localized minimum (maximum) of the GS fidelity F (its susceptibility S) to define the crossover. In other words, the GS fidelity and its susceptibility signal precursors of the crossover from two-site to singlet-site bipolarons.

To illustrate the ground-state configurations in these two regimes, we calculate the GS wavefunction for phonons, which can be described in the x representation by using the phonon

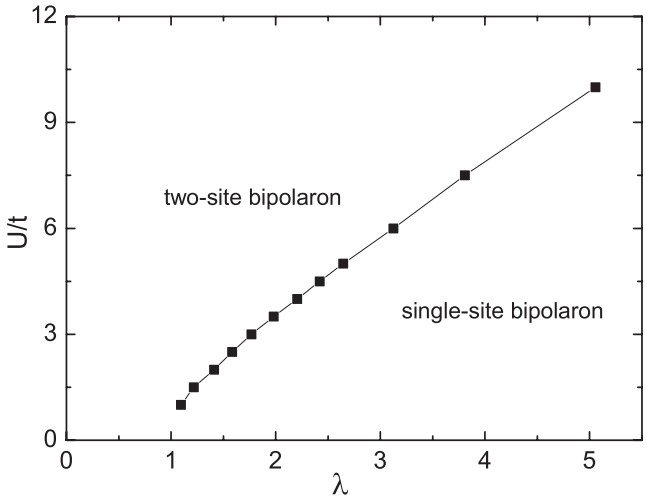

Figure 4. The crossover from two-site to single-site-dominated bipolaron is displayed by the U/t–λ phase diagram according to the localized minimum (maximum) of the fidelity (its susceptibility) for $V = 0.2$, $t = 2.0$, $\varepsilon = 0.8$.

Fock state

$$|N\rangle_{\rm ph} = \sqrt{\frac{1}{\sqrt{\pi}2^N N!}} e^{-x^2/2} H_N(x),$$

with $H_N(x)$ the Hermite polynomials of order N. According to equation (5), we plot the probability distribution ρ_1, ρ_2 and ρ_3 of phonons where two electrons are at single site 1, single site 2 and two sites for $\lambda = 1$ and 2.5 in figure 5. Here $U = 3.0$ and the other parameters are the same as those in figure 4. The probability distribution of phonons for both pure two-site bipolarons and single-site bipolarons are symmetric with the zero point. As shown in figure 4, $\lambda = 1$ is in the two-site bipolaron regime, while $\lambda = 2.5$ is in the single-site bipolaron

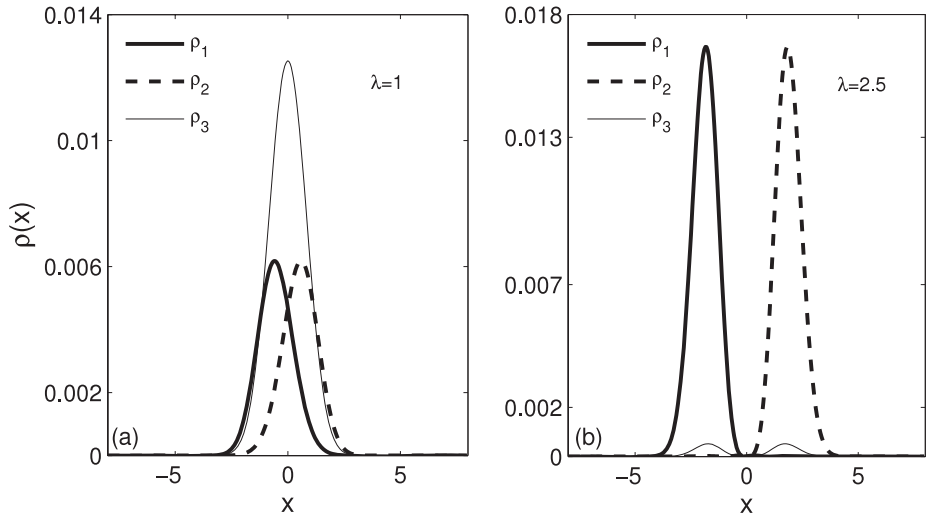

Figure 5. The probability distribution of the phonons for (a) $\lambda = 1$ and (b) $\lambda = 2.5$. $U = 3.0$ and the other parameters are the same as those in figure 4.

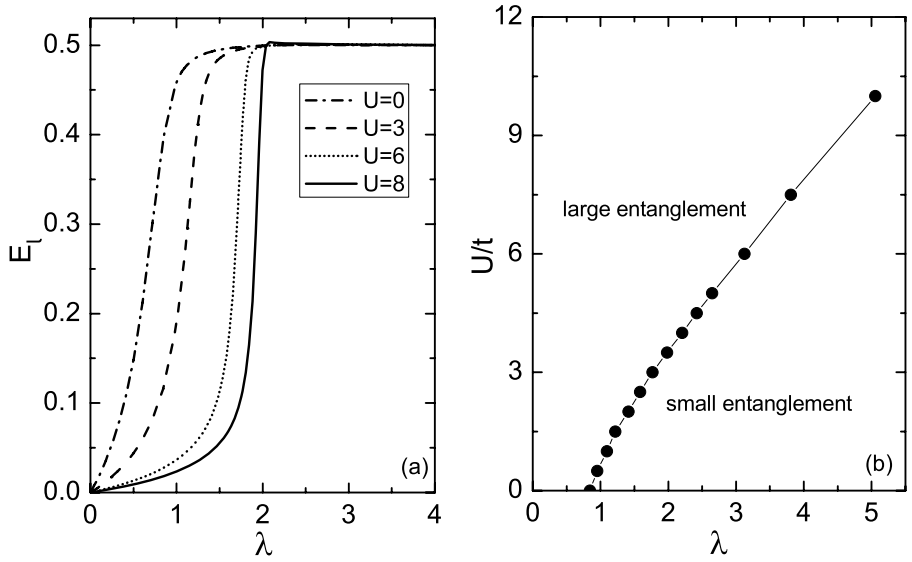

Figure 6. (a) Linear entropy E_l versus λ for $U = 0$, 3, 6 and 8. The maximum $E_l = 0.5$ corresponds to the single-site bipolaron in a strong coupling region. (b) The U/t–λ line is the edge of the cliff which separates the large and small entanglement regions. In all cases $V = 0.2$, $t = 2.0$ and $\varepsilon = 0.8$.

regime. The probability distribution of phonons for pure two-site bipolarons takes the Gaussian-like form displaced from the zero point at $\lambda = 1$ and splits into two small peaked ones at $\lambda = 2.5$. The probability distribution of phonons for single-site bipolarons takes the Gaussian-like form displaced from a nonzero point at the two-site bipolaron regime ($\lambda = 1$). It becomes larger at the single-site bipolaron regime ($\lambda = 2.5$).

Moreover, the character of the entanglement entropy can be used effectively to examine its relation to the interplay between the e–ph interaction and e–e Coulomb repulsion. Here, the linear entropy E_l [36, 39, 37] is an alternative measurement for the entanglement between electrons and their phonon environment, which is a linearized version of the von Neumann entropy. Its definition is

$$E_l = 1 - \mathrm{Tr}\rho^2, \tag{10}$$

where $\rho = \mathrm{Tr}(|\psi\rangle\langle\psi|)$ is the reduced density matrix of electrons by taking a partial trace over the phonon degrees of freedom. Attributed to the normalized GS wavefunction $|\psi\rangle$ of the singlet bipolaronic state in equation (5), the linear entropy can be derived simply as

$$E_l = 1 - [\langle\varphi_1|\varphi_1\rangle^2 + \langle\varphi_2|\varphi_2\rangle^2 + \langle\varphi_3|\varphi_3\rangle^2 + 2\,\mathrm{Re}(\langle\varphi_1|\varphi_2\rangle^2 + \langle\varphi_1|\varphi_3\rangle^2 + \langle\varphi_2|\varphi_3\rangle^2)]. \tag{11}$$

As plotted in figure 6(a), the linear entropy E_l increases smoothly with the e–ph coupling parameters λ in the origin and then reaches a constant 0.5 for $U = 0, 3, 6$ and 8. Obviously there is an occurrence of the crossover regime in the intermediate coupling regime, which shifts to larger λ with increasing U. Similar crossover behavior has been demonstrated by the GS fidelity F and its susceptibility. In

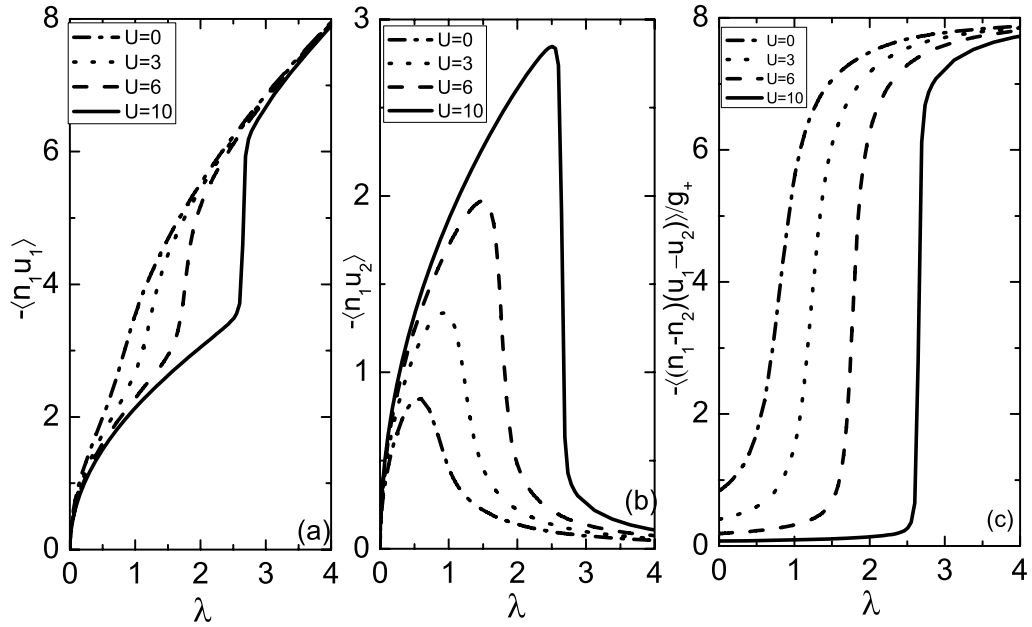

Figure 7. Correlation function versus λ (a) $-\langle n_1u_1\rangle$, (b) $-\langle n_1u_2\rangle$ and (c) $-\langle(n_1-n_2)(u_1-u_2)\rangle/g_1$ for $U=0$, 3, 6 and 10 by choosing $V=0.2$, $t=2.0$ and $\varepsilon=0.8$. A more abrupt crossover occurs for larger $U=10$ (solid line).

general, in the weak e–ph coupling region, each electron is dressed with phonons of its own site and form a so-called two-site-dominated bipolaron. It leads to the degree of the e–ph entanglement increase with the e–ph interaction λ. Meanwhile it is suppressed by the on-site Coulomb repulsions U. Consequently, the linear entropy E_1 describes the intrinsic competition between the e–ph interaction and e–e Coulomb repulsion. As λ exceeds the crossover regime, the e–ph interaction dominates and the entire charge of the electrons and entire deformations of the lattices are restricted on one site. As a result, the single-site bipolarons are maximally entangled $E_1=0.5$, independent of λ and U, in the strong coupling region. Figure 6(b) shows that the U/t–λ line is the edge of the cliff which separates the large and small entanglement regions. Therefore we can say that, in the presence of quantum correlations, the two-site (singlet-site) bipolarons are effectively characterized by the low (high) degree of bipartite quantum entanglement.

Some correlation functions may be closely related to the entanglement entropy [38, 39]. Naturally, we seek classically to discuss this crossover by means of the static on-site and inter-site correlation functions $\langle n_1u_1\rangle$ and $\langle n_1u_2\rangle$, which reveal the spatial extent of lattice deformations induced by electrons, respectively. The u_i denotes the lattice deformations on site i produced by the electrons and n_i is the number operator of the electrons. The GS correlation functions are written as [34, 40]

$$\langle n_1u_{1,2}\rangle=\frac{n_1}{2}\langle\pm(d+d^\dagger)-2g_1n\rangle. \tag{12}$$

The positive (negative) sign is associated with $\langle n_1u_1\rangle$ and $\langle n_1u_2\rangle$, respectively. By using the exact GS wavefunction of the singlet bipolaronic state obtained above, the correlation functions equation (12) can be expressed as follows:

$$\begin{aligned}\langle n_1u_1\rangle=&-2g_1\sum_{m=0}^{N}(2c_m^2+f_m^2)+\sum_{m=1}^{N}\sqrt{m}(c_m^*c_{m-1}\\&+0.5f_m^*f_{m-1})+\sum_{m=0}^{N-1}\sqrt{m+1}(c_m^*c_{m+1}\\&+0.5f_m^*f_{m+1}).\end{aligned} \tag{13}$$

$$\begin{aligned}\langle n_1u_2\rangle=&-2g_1\sum_{m=0}^{N}(2c_m^2+f_m^2)-\sum_{m=1}^{N}\sqrt{m}(c_m^*c_{m-1}\\&+0.5f_m^*f_{m-1})-\sum_{m=0}^{N-1}\sqrt{m+1}(c_m^*c_{m+1}\\&+0.5f_m^*f_{m+1}).\end{aligned} \tag{14}$$

The functions $-\langle n_1u_1\rangle$ and $-\langle n_1u_2\rangle$ against the e–ph coupling strength λ are plotted in figures 7(a) and (b). One can observe that $-\langle n_1u_1\rangle$ and $-\langle n_1u_2\rangle$ increase monotonically with λ in the weak coupling regime. When λ exceeds a critical value, $-\langle n_1u_1\rangle$ and $-\langle n_1u_2\rangle$ show different behaviors. A continuous change in the curvature of $-\langle n_1u_2\rangle$ is the transition point in the crossover region, the so-called crossover point, where $-\langle n_1u_2\rangle$ reaches its maximum in figures 7(b). It leads to the result that the singlet-site bipolaron and the two electrons are localized on one site in the strong coupling region. Thus the e–ph interaction is the dominant effect and corresponds to the maximal entanglement of the singlet-site bipolaron, as shown in figure 6(a).

The nature of the crossover from the two-site to single-site bipolarons can be well marked by the correlation function $\langle(n_1-n_2)(u_1-u_2)\rangle/g_1$, where the results are presented in figure 7(c). It is observed obviously that the two-site bipolaron regime of the coupling strength λ is wider for larger U in the weak e–ph coupling regime and the critical point value of λ

shifts to the right regime where a crossover occurs. The results are consistent with the above behavior of the GS entanglement.

4. Conclusions

In this work we have solved exactly the two-site Hubbard–Holstein model by the extended phonon coherent state approach. Indicator properties, such as the double occupancy probability, the drop of the fidelity and the incremental entanglement entropy are employed to locate two-site- and single-site-dominated bipolaron regions, displaying an occurrence of crossover. We use the localized minimum of the fidelity to define a crossover and plot the bipolaron phase diagram, which separates the large and small entanglement regions. We demonstrate the relation between the entanglement and correlation function, the large e–ph entanglement corresponding to the large magnitude of lattice deformations. It found that the e–ph interaction and the e–e Coulomb repulsion have opposite effects on the two-site-to single-site-dominated bipolaron transition in this two-site HH bipolaron system. The similar bipolaron crossover behaviors are also observed classically in the static correlation function. This study on the basis of exact solutions may provide some insights into the more complicated Hubbard–Holstein systems in a infinite chain where the exact solution is hard to obtain.

Acknowledgments

This work was supported by the National Natural Science Foundation of China, PCSIRT (grant no. IRT0754) in the University in China, the National Basic Research Program of China (grant no. 2009CB929104), the Zhejiang Provincial Natural Science Foundation under grant no. Z7080203 and the Program for Innovative Research Team in Zhejiang Normal University.

References

[1] Hill S and Wootters W K 1997 *Phys. Rev. Lett.* **78** 26
[2] Wootters W K 1998 *Phys. Rev. Lett.* **80** 10
[3] Vidal G, Latorre J I, Rico E and Kitaev A 2003 *Phys. Rev. Lett.* **90** 227902
[4] Gu S J, Deng S S, Li Y Q and Lin H Q 2004 *Phys. Rev. Lett.* **93** 086402
[5] Chen Q H, Zhang Y Y, Liu T and Wang K L 2008 *Phys. Rev.* A **78** 051801
[6] Quan H T, Song Z, Liu X F, Zanardi P and Sun C P 2006 *Phys. Rev. Lett.* **96** 140604
[7] Buonsante P and Vezzani A 2007 *Phys. Rev. Lett.* **98** 110601
[8] Chen S, Wang L, Hao Y J and Wang Y P 2008 *Phys. Rev.* A **77** 032111
[9] Zanardi P and Paunković N 2006 *Phys. Rev.* E **74** 0331123
[10] Buonsante P and Vezzani A 2007 *Phys. Rev. Lett.* **98** 110601
[11] Yang M F 2007 *Phys. Rev.* B **76** 180403
[12] You W L, Li Y W and Gu S J 2007 *Phys. Rev.* E **76** 022101
Chen S, Wang L, Gu S J and Wang Y 2008 *Phys. Rev.* E **76** 061108
[13] Dunning C, Links J and Zhou H Q 2005 *Phys. Rev. Lett.* **94** 227002
[14] Oelkers N and Links J 2007 *Phys. Rev.* B **75** 115119
[15] Liu T, Zhang Y Y, Chen Q H and Wang K L 2009 *Phys. Rev.* A **80** 023810
[16] Khan A and Pieri P 2009 *Phys. Rev.* A **80** 012303
[17] Vidal J *et al* 2004 *Phys. Rev.* A **69** 054101
[18] Das A N and Choudhury P 1994 *Phys. Rev.* B **49** 13219
[19] Anfossi A *et al* 2005 *Phys. Rev. Lett.* **95** 056402
[20] Cozzini M, Giorda P and Zanardi P 2007 *Phys. Rev.* B **75** 014439
[21] Clay R T and Hardikar R P 2005 *Phys. Rev. Lett.* **95** 096401
[22] Tezuka M, Arita R and Aoki H 2005 *Phys. Rev. Lett.* **95** 226401
[23] Ning W Q, Zhao H, Wu C Q and Lin H Q 2006 *Phys. Rev. Lett.* **96** 156402
[24] Fehske H, Hager G and Jeckelmann E 2008 *Europhys. Lett.* **84** 57001
[25] Fehske H, Wellein G, Loos J and Bishop A R 2008 *Phys. Rev.* B **77** 085117
[26] Wellein G, Röder H and Fehske H 1996 *Phys. Rev.* B **53** 9666
[27] Bonča J and Trugman S A 2001 *Phys. Rev.* B **64** 094507
[28] Das A N and Choudhury P 1994 *Phys. Rev.* B **49** 18
[29] Acquaroneet M *et al* 1998 *Phys. Rev.* B **58** 7626
[30] Ranninger J and Thibblin U 1992 *Phys. Rev.* B **45** 7730
[31] de Mello E V L and Ranninger J 1997 *Phys. Rev.* B **55** 14872
[32] Berciu M 2007 *Phys. Rev.* B **75** 081101(R)
[33] Chen Q H *et al* 1996 *Phys. Rev.* B **53** 11296
[34] Han R S, Lin Z J and Wang K L 2002 *Phys. Rev.* B **65** 174303
[35] Wang K L, Liu T and Feng M 2006 *Eur. Phys. J.* B **54** 283
[36] Zhao Y, Zanardi P and Chen G H 2004 *Phys. Rev.* B **70** 195113
[37] Wang X and Sanders B 2005 *J. Phys. A: Math. Gen.* **38** 67
[38] Glaser U, Büttner H and Fehske H 2003 *Phys. Rev.* A **68** 032318
[39] Stojanović V M and Vanević M 2008 *Phys. Rev.* B **78** 214301
[40] Chatterjee J and Das A N 2000 *Phys. Rev.* B **61** 4592